



HAL
open science

Paleogene clockwise tectonic rotation of the Xining-Lanzhou region, northeastern Tibetan Plateau

Guillaume Dupont-Nivet, B. Horton, R. Butler, J. Wang, J. Zhou, G. Waanders

► **To cite this version:**

Guillaume Dupont-Nivet, B. Horton, R. Butler, J. Wang, J. Zhou, et al.. Paleogene clockwise tectonic rotation of the Xining-Lanzhou region, northeastern Tibetan Plateau. *Journal of Geophysical Research: Solid Earth*, 2004, 109 (B4), 10.1029/2003JB002620 . hal-02957162

HAL Id: hal-02957162

<https://hal.science/hal-02957162v1>

Submitted on 5 Oct 2020

HAL is a multi-disciplinary open access archive for the deposit and dissemination of scientific research documents, whether they are published or not. The documents may come from teaching and research institutions in France or abroad, or from public or private research centers.

L'archive ouverte pluridisciplinaire **HAL**, est destinée au dépôt et à la diffusion de documents scientifiques de niveau recherche, publiés ou non, émanant des établissements d'enseignement et de recherche français ou étrangers, des laboratoires publics ou privés.

Paleogene clockwise tectonic rotation of the Xining-Lanzhou region, northeastern Tibetan Plateau

G. Dupont-Nivet,^{1,2} B. K. Horton,¹ R. F. Butler,³ J. Wang,⁴ J. Zhou,⁵ and G. L. Waanders⁶

Received 11 June 2003; revised 2 December 2003; accepted 10 December 2003; published 1 April 2004.

[1] To help understand the deformational history of the northeastern Tibetan Plateau, paleomagnetic samples were collected from 177 sites and two magnetostratigraphic sections at 16 localities distributed among Upper Jurassic-Lower Cretaceous to Pliocene sedimentary and subordinate volcanic rocks within the Xining-Lanzhou region (34–37°N, 101–105°E). A total of 127 sites at 12 localities yielded primary magnetizations confirmed by fold, reversal, and conglomerate tests. Age control on sedimentary rocks is provided by regional synthesis of chronostratigraphic data and our own biostratigraphic and magnetostratigraphic analysis presented in the companion paper by *Horton et al.* [2004]. Analysis of paleomagnetic declination combined with results from previous studies yield a remarkably consistent trend of vertical axis tectonic rotations across the studied region. Whereas $19.0 \pm 7.2^\circ$ to $37.8 \pm 10.6^\circ$ clockwise rotations are recorded consistently in all paleomagnetic localities in Lower Cretaceous to Eocene rocks, all paleomagnetic localities in Oligocene to Pliocene rocks have recorded minor to insignificant rotations, indicating that the Xining-Lanzhou region has undergone a wholesale regional clockwise rotation during late Paleogene time. Consistent with regional chronostratigraphic and thermochronologic results, this late Paleogene tectonic rotation confirms that deformation reached regions of the northern Tibetan Plateau shortly after the initial collision of India with Asia. When compared to rotational paleomagnetic results from adjacent regions, several mechanisms can be proposed to explain the clockwise rotation. On the basis of consistency with geologic data we prefer a model involving clockwise rotation of the Xining-Lanzhou region through right-lateral shear, and associated shortening, related to northward indentation of the Qaidam basin. **INDEX TERMS:** 1525 Geomagnetism and Paleomagnetism: Paleomagnetism applied to tectonics (regional, global); 8102 Tectonophysics: Continental contractional orogenic belts; 9320 Information Related to Geographic Region: Asia; 9604 Information Related to Geologic Time: Cenozoic; **KEYWORDS:** tectonics, paleomagnetism, Tibetan Plateau

Citation: Dupont-Nivet, G., B. K. Horton, R. F. Butler, J. Wang, J. Zhou, and G. L. Waanders (2004), Paleogene clockwise tectonic rotation of the Xining-Lanzhou region, northeastern Tibetan Plateau, *J. Geophys. Res.*, 109, B04401, doi:10.1029/2003JB002620.

1. Introduction

[2] The Cenozoic deformation of Asia is dominated by the effects of the Indo-Asia collision, which resulted in the construction of the Tibetan Plateau [*Argand*, 1924; *Besse and Courtillot*, 1988; *Le Pichon et al.*, 1992; *Molnar and Tapponnier*, 1975; *Yin and Harrison*, 2000]. The spatial and temporal evolution of this deformation is essential to

understanding lithospheric behavior during continental collision and the mechanisms of plateau uplift and their influence on global climate change [*DeCelles et al.*, 2002; *Mattauer et al.*, 1999; *Royden*, 1996; *Ruddiman et al.*, 1989]. Despite the growing geological data set, several first-order questions remain. Is the deformation distributed over the Himalayan-Tibetan orogen or localized on major lithospheric scale faults allowing eastward extrusion [*England and Houseman*, 1988; *Peltzer and Tapponnier*, 1988]? Did uplift of the Tibetan Plateau migrate progressively northward since the onset of collision [*Tapponnier et al.*, 2001] or altogether in the late Miocene in response to convective removal of Asian lithosphere [*Molnar et al.*, 1993]? These various tectonic models make testable predictions for the kinematic evolution of the orogen. Using geodetic analysis [e.g., *Bendick et al.*, 2000; *Chen et al.*, 2000; *Shen et al.*, 2001], earthquake moment tensor analysis [e.g., *Holt and Haines*, 1993; *Molnar and Lyon-Caen*, 1989], seismotectonics, and Quaternary offset of geomorphic features [e.g., *Lasserre et al.*, 2002; *Peltzer et al.*, 1989; *van der Woerd et al.*, 1998; *Washburn et al.*, 2004],

¹Department of Earth and Space Sciences, University of California, Los Angeles, California, USA.

²Now at Faculty of Earth Sciences, Paleomagnetic Laboratory—"Fort Hoofdijk," Utrecht University, Utrecht, Netherlands.

³Department of Geosciences, University of Arizona, Tucson, Arizona, USA.

⁴Institute of Geochemistry, Chinese Academy of Sciences, Guangzhou, China.

⁵Faculty of Earth Sciences, China University of Geosciences, Wuhan, China.

⁶Waanders Palynology, Encinitas, California, USA.

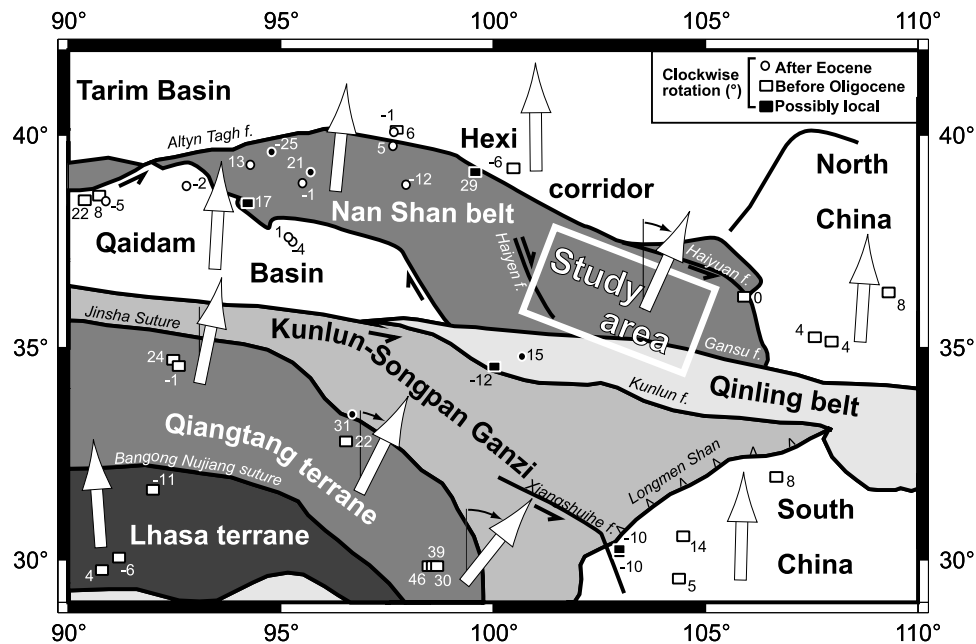


Figure 1. Regional map of the eastern Tibetan Plateau and adjacent region showing major tectonic features. White box indicates location of study area. Locations of previous paleomagnetic studies are shown by squares (pre-Oligocene rocks) and circles (post-Eocene rocks) with adjacent number indicating calculated vertical axis clockwise rotation with respect to the APWP of Eurasia [Besse and Courtillot, 2002] (using the rotation value, each result can be identified in Table A14). Black symbols indicate paleomagnetic localities possibly affected by rotation of local structures. Large arrows indicate arithmetic mean vertical axis rotation averaged over broader region.

contemporaneous to Quaternary stress and displacement distribution have been determined. Clearly, these kinematic constraints of broad geographic extent cannot be extrapolated back to describe the deformation since the onset of collision [England and Molnar, 1997; Holt et al., 2000; Peltzer and Saucier, 1996]. Fortunately, long-term deformational information is recorded within the Jurassic to Quaternary sedimentary successions throughout the Tibetan Plateau and adjacent regions. Structural and stratigraphic analyses have quantified deformation histories and provided direct kinematic constraints [e.g., Bally et al., 1986; Burbank et al., 1996; DeCelles et al., 1998, 2002; Horton et al., 2002; Ratschbacher et al., 1996; Ritts and Biffi, 2000, 2001; D. M. Robinson et al., 2002; Yin et al., 2002]. Analyses of paleomagnetic declinations recorded in these sedimentary rocks have provided the net vertical axis rotation of crustal fragments revealing important constraints such as bending of the Himalayan arc [Klootwijk et al., 1985], Cenozoic clockwise rotation of the Indochina block [Sato et al., 2001; Yang and Besse, 1993], clockwise and counterclockwise rotation at the eastern and western margins of the Tibetan Plateau [Huang et al., 1992; Otofujii et al., 1990; Thomas et al., 1993, 1994], and the absence of rotation of the northeastern Tibetan Plateau since Oligocene time [Dupont-Nivet et al., 2002, 2003]. An important challenge, and limitation, of these studies concerns the ability to provide age control on the sedimentary rocks.

[3] In this study we report paleomagnetic results from the Xining-Lanzhou region at the northeastern edge of the Tibetan Plateau (Figure 1). Previous paleomagnetic studies in the Xining-Lanzhou region indicate post-Early Creta-

ceous clockwise rotations on the order of 20° – 40° [Halim et al., 1998; Yang et al., 2002]. Because the Xining-Lanzhou region is affected by documented Miocene to Pliocene deformation [Burchfiel et al., 1991; Gaudemer et al., 1995; Lasserre et al., 2002; Meyer et al., 1998; Zhang et al., 1990], these rotations have been attributed to recent tectonics and rotational extrusion of the entire northeastern Tibetan Plateau including the Qaidam basin [Chen et al., 2002a]. However, no significant rotations are observed in the Qaidam basin since Oligocene time [Dupont-Nivet et al., 2002]. In this paper, we present a broad paleomagnetic data set that constrains the timing and the spatial extent of tectonic rotations in the Xining-Lanzhou region, yielding implications for the rotational history of the northeastern Tibetan Plateau and the development of the Indo-Asia collision system.

2. Methods

[4] Paleomagnetic sampling was performed using methods referenced by Butler [1992]. We apply the term paleomagnetic locality to an area (usually with dimensions $<10 \text{ km}^2$) from which paleomagnetic sites were collected within one or several stratigraphic sections or volcanic sequences. At each site (a single sedimentary horizon or volcanic flow), eight oriented core samples were collected and bedding attitude was measured. When performing magnetostratigraphic analysis [see Horton et al., 2004], two to four samples were collected per magnetostratigraphic level (a single sedimentary horizon). All samples were stored, thermally demagnetized and measured in a magnet-

ically shielded room with average field intensity below 200 nT. After initial measurement of natural remanent magnetization, samples were thermally demagnetized at 10–20 temperature steps from 50°C to 700°C. Results from at least four successive temperatures were analyzed by principal component analysis [Kirschvink, 1980] to determine sample characteristic remanent magnetization (ChRM) directions. Samples yielding maximum angular deviation $>15^\circ$ were rejected from further analysis. Site-mean ChRM directions were calculated using methods of Fisher [1953]. Sample ChRM directions more than two angular standard deviations from the initial site-mean direction were rejected prior to final site-mean calculation. Sites with less than four sample ChRM directions and site-mean directions with $\alpha_{95} > 25^\circ$ were rejected. In magnetostratigraphic sections, 5–11 sample ChRM directions from two to eight successive magnetostratigraphic levels were gathered to calculate site-mean directions for tectonic analysis. Locality-mean directions were calculated by applying Fisher [1953] statistics to the set of normal polarity site-mean directions and antipodes of reversed polarity site-mean directions from each locality (discarding site means more than two angular standard deviations from the preliminary mean). The expected direction at a paleomagnetic locality was calculated using the appropriate age reference paleomagnetic pole for Eurasia from Besse and Courtillot [2002]. Concordance/discordance calculations followed the methods of Beck [1980] and Demarest [1983].

3. Paleomagnetic Results

[5] A total of 1703 paleomagnetic samples (177 sites) were collected at 16 paleomagnetic localities distributed across the Xining-Lanzhou region (34–37°N, 101–105°E) at the northeastern edge of the Tibetan Plateau (Figure 2). Sampling was performed in two general basin systems: four paleomagnetic localities in the Dangchang basin in the western Qinling belt, between the Kunlun and the Gansu fault systems and 12 paleomagnetic localities from the large Xining-Minhe-Longzhong basin complex within the region situated between the Gansu and Haiyuan fault systems (Figure 1). Age control on the collected sedimentary rocks is provided by the companion study by Horton *et al.* [2004], in which a compilation of existing regional chronostratigraphic data is supplemented and improved by new constraints from palynomorph assemblages and magnetostratigraphic sampling within measured stratigraphic sections.

3.1. Dangchang Basin

[6] Detailed stratigraphic analysis of the Cretaceous Dangchang basin and the Paleogene Nanyang and Niuding Shan basins was performed in combination with this study and is described by Horton *et al.* [2004]. Paleomagnetic sampling in the Dangchang basin is divided in four parts: (1) magnetostratigraphic sampling near Dangchang, (2) the Nanyang basin, (3) the Niuding Shan basin, and (4) basaltic rocks throughout the Nanyang and Niuding Shan regions (Figure 3).

3.1.1. Dangchang Paleomagnetic Locality

[7] The ~ 3 -km-thick basal part of the Dangchang basin is exposed in a regional northwest-southeast trending syncline with gentle northwest plunge. This succession is principally

composed of alluvial fan deposits of the Mogou and Chela Formations that were originally mapped as Paleogene (Map I-48-XV (Minxian), 1:200,000 [Qinghai Bureau of Geology and Mineral Resources (QBGM), 1991]) but more recently attributed a broadly Cretaceous age based on limited paleontologic constraints [QBGM, 1985]. An Aptian-Albian age is assigned to these successions by our own palynological samples [Horton *et al.*, 2004].

[8] We collected 85 magnetostratigraphic levels (at three samples per levels) in a homoclinal 1500-m-thick section, supplemented by 8 separate sites (at eight samples per site; see auxiliary material Table A1¹) within broadly folded parts of the section in order to perform a fold test. Upon demagnetization of one sample per magnetostratigraphic level, all samples yielded ChRM directions of normal polarity direction (auxiliary material Figure A1) such that demagnetization of the remaining samples from the magnetostratigraphic sampling was unnecessary to assess polarity distribution. For tectonic analysis, sample ChRM directions from seven to eight successive magnetostratigraphic levels were gathered into 10 site-mean directions and added to the eight site-mean directions from folded part of the section to calculate the overall mean direction. Negligible direction variation ($\sim 2^\circ$) due to plunge correction is within the 95% confidence limit and not considered in further analysis. These 18 directions pass the fold test [McFadden, 1990] indicating a pre-folding origin for the ChRM. Although the lack of reverse polarity directions throughout the section precludes the application of the reversals test, the uniform normal polarity is in agreement with the Aptian-Albian fossil assemblages that indicate deposition during the Cretaceous normal polarity superchron.

3.1.2. Nanyang and Niuding Shan Paleomagnetic Localities

[9] The Nanyang and Niuding Shan basins are exposed in narrow east-west trending synclines consisting of 100- to 200-m-thick, moderately consolidated proximal sedimentary rocks (Figure 3). Previous mapping did not distinguish them from the Early Cretaceous alluvial fan deposits of the basal Dangchang succession described above and confer them either a Cretaceous age [QBGM, 1985] or a Paleogene age (Map I-48-XV (Minxian), 1:200,000 [QBGM, 1991]). The Paleogene age assignment is favored by the distinctive lithological, provenance and structural setting of these strata characteristics of the western Qinling Shan basins such as the Lixian and the Paleogene Zhangxian basins [Horton *et al.*, 2004; Zhai and Cai, 1984]. Furthermore, the Paleogene age is preferred because early Miocene basalts concordantly overlie sedimentary rocks of the Nanyang and Niuding Shan basins (see section 3.1.3).

[10] Within the Nanyang basin, we collected six sites (Table A2) from red fine-grained sandstones at separate locations with different bedding attitudes. Four of the six sites yielded interpretable ChRM directions. As illustrated in Figure A2, site-mean directions tightly cluster after structural correction, passing the fold test [McFadden, 1990] and indicating a pre-folding origin for the ChRM.

¹Auxiliary material is available at <ftp://ftp.agu.org/apend/jb/2003JB002620>.

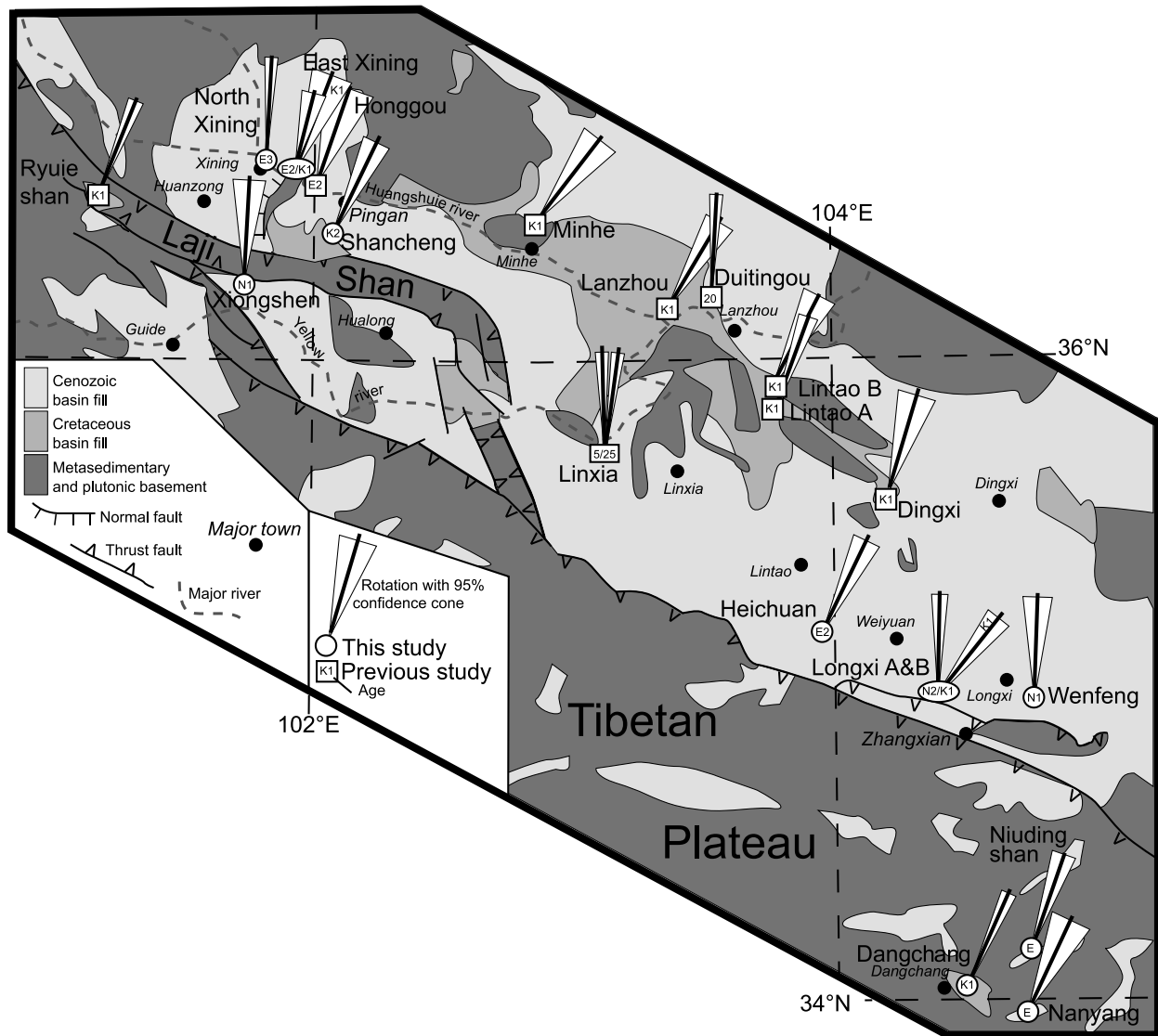


Figure 2. Simplified geologic map of the Xining-Lanzhou region showing vertical axis rotation with respect to the APWP of Eurasia [Besse and Courtillot, 2002] (locality results on Table 1). The age of the sampled rocks is indicated (in Ma) if known with enough precision; otherwise, the series symbols of the international stratigraphic chart are used (K1, Early Cretaceous; K2, Late Cretaceous; E, Paleogene; E1, Paleocene; E2, Eocene; E3, Oligocene; N1, Miocene; N2, Pliocene).

[11] Eight sites were collected within the Niuding Shan basin at separate locations with different bedding attitudes (Table A3). Sampled lithologies include red fine-grained sandstone and mudstone, except for one site (ND009), where samples were collected from eight different sedimentary clasts within a matrix-supported conglomerate. The seven sites consisting of fine-grained red beds yielded interpretable ChRM directions. Clustering of site-mean direction after structural correction (Figure A3) indicate a positive fold test [McFadden, 1990] and a ChRM acquired before folding. Five of the eight samples from conglomerate clasts yielded interpretable ChRM directions of random orientation, as expected for a positive conglomerate test (Figure A3c). Collectively, these field tests indicate a primary origin for the magnetization in the Niuding Shan basin.

3.1.3. Basalts of the Nanyang and Niuding Shan Regions

[12] Collected basaltic rocks are part of an igneous complex consisting of flows concordantly overlying successions of the Nanyang and Niuding Shan basins, or locally, of shallow level intrusions cutting basinal and prebasinal rocks. Our ongoing analysis of a suite of volcanic samples throughout the region (including $^{40}\text{Ar}/^{39}\text{Ar}$ whole rock dating at UCLA and isotopic analyses at the Guangzhou Institute of Geochemistry) has provided six weighted-mean ages (25.0 ± 0.6 Ma, 24.1 ± 0.3 Ma, 22.6 ± 0.2 Ma, 19.8 ± 0.3 Ma, 19.3 ± 0.8 Ma, and 14.5 ± 0.7 Ma). These dates constrain the age of the volcanic complex and provide a minimum age for the fill of the Nanyang and Niuding Shan basins.

[13] Seven paleomagnetic sites were collected within three basaltic flows concordantly overlying sedimentary

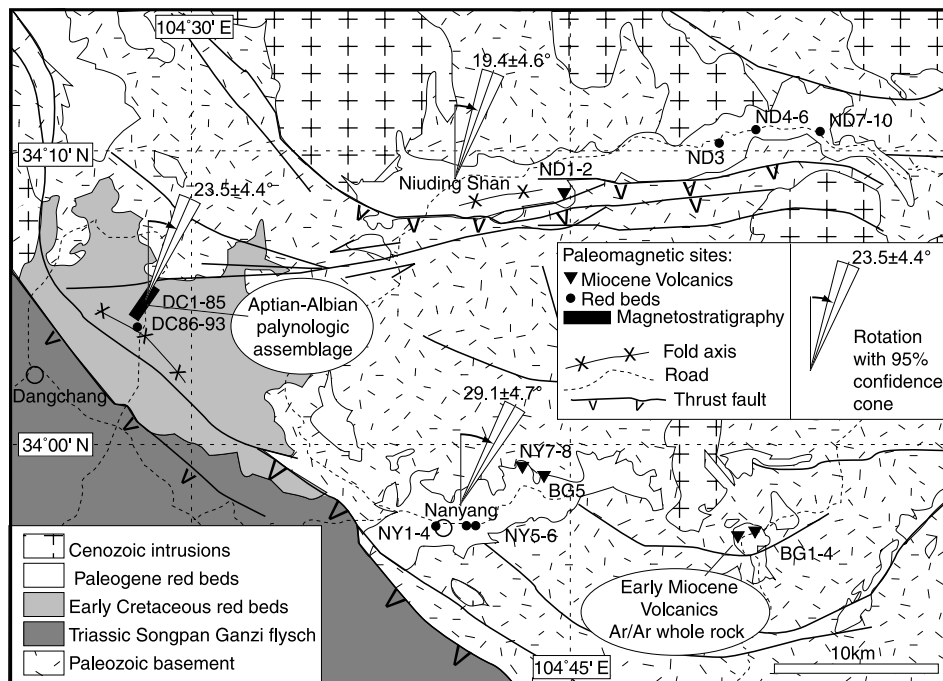


Figure 3. Simplified geologic map of the Dangchang area with sampling locations (with site identification numbers) and mean vertical axis rotations with respect to the APWP of Eurasia [Besse and Courtillot, 2002] for the Dangchang, the Nanyang, and the Niuding Shan localities.

rocks of the Niuding Shan (sites ND001 and ND002) and Nanyang basins (BG001-BG005) and one site within a dike intruding red beds of the Nanyang basin (NY007; see Table A4). Sampled volcanic rocks are fine-grained massive basalts with small olivine inclusions that were carefully avoided. Bedding orientations of underlying strata were used to correct for structural disturbance of the volcanic rocks. When restoring to horizontal, site-mean directions clearly scatter, probably indicating a postfolding origin for the ChRM (Figure A4). All sites have reverse polarity direction that average in geographic coordinates to a southerly direction ($N180.0^\circ$) with shallow inclination (35.3°). These results suggest recent remagnetization of the collected basalts, although the processes responsible remain unclear. Because the timing of acquisition of the ChRM is not clear, we do not consider the ChRM directions obtained from these rocks for further tectonic analysis.

3.2. Xining-Minhe-Longzhong Basin Complex

[14] The Late Jurassic to Tertiary Xining-Minhe-Longzhong basin complex comprises the larger part of the study region in the northeastern Tibetan Plateau (Figure 2). As described by Horton *et al.* [2004] the Xining-Minhe basin developed originally during Late Jurassic-Early Cretaceous time, possibly related to an initial phase of extension followed by thermal subsidence during the early Tertiary. During mid to late Tertiary time the Xining-Minhe basin was segmented into several subbasins, collectively referred to as the Longzhong basin [Zhai and Cai, 1984]. In sections 3.2.1–3.2.8, we present the results from 12 paleomagnetic localities along an east to west transect across the study area.

3.2.1. Gangu Paleomagnetic Locality

[15] At the eastern part of our sampling area, 3 km south of the town of Gangu, extensive exposures of alluvial fan deposits are broadly mapped as Paleogene (Map I-48-X (Taian), 1:200,000 [Gansu Bureau of Geology and Mineral Resources (GBGMR), 1989; Zhai and Cai, 1984]). Within a >200-m-thick, gently south dipping section, six sites were collected in medium-grained sandstones with a fine orange matrix at the following location: $34^\circ43.20'$; $105^\circ19.58'$. Upon thermal demagnetization of two pilot samples per site, erratic demagnetization behavior with low intensity of magnetization prevented interpretation of ChRM directions.

3.2.2. Wenfeng Paleomagnetic Locality

[16] Near the village of Wenfeng and along the road from Longxi to Wushan, eight sites were collected in light brown to red clay-rich mudstones (Table A5) within a 250-m-thick subhorizontal section. This succession is broadly mapped as Neogene based on regional stratigraphic correlations (Map I-48-IX (Longxi), 1:200,000 [GBGMR, 1989]). On the basis of the disconformably overlying Pliocene to Quaternary conglomerates [Liu *et al.*, 1998] and lithologic similarity to the regionally well-documented Miocene red clay deposits [Ding *et al.*, 2001], we tentatively attribute a Miocene age to the sampled section.

[17] Seven sites yielded interpretable ChRM directions. Application of the reversals test of McFadden and McElhinny [1990] yields an indeterminate result. However, the one site-mean direction of reverse polarity is statistically indistinguishable from the antipodal mean direction of the other six normal polarity sites suggesting magnetization acquired during or shortly after deposition (Figure A5).

3.2.3. Zhangxian Paleomagnetic Locality

[18] Within a >500-m-thick section mapped broadly as Neogene (Map I-48-IX (Longxi), 1:200,000 [GBGMR, 1989]) and dipping gently to the south, six sites were collected in variegated dark red to light orange sandstones and mudstones. The site is located along the main river a few kilometers to the southeast of the city of Zhangxian (N34°48.94'; E104°31.16'). Upon demagnetization of two pilot samples per site, erratic demagnetization behavior and low intensity of magnetization preclude interpretation of ChRM directions.

3.2.4. Longxi-A Paleomagnetic Locality

[19] Within a canyon along the main road from Zhangxian to Longxi, a few kilometers north of the village of Shanca, six sites were collected in red, well-indurated, fine-grained sandstones to siltstones (Table A6) within a ~150-m-thick folded section. The succession is broadly mapped as Cretaceous (Map I-48-IX (Longxi) 1:200,000 [GBGMR, 1989]). Lithologies and facies throughout these successions are similar to sampled successions of the Hekou group [Yu *et al.*, 2001], leading us to tentatively attribute an Early Cretaceous age for the sampled section. We observed signs of previous paleomagnetic sampling at approximately 15 sites in this section, but we are unaware of any referrals to this sampling in the literature. All six sites yielded interpretable ChRM directions for which pre-folding acquisition of the magnetization is demonstrated by clear clustering of site-mean directions after structural correction (Figure A6) defining a positive fold test [McFadden, 1990].

3.2.5. Longxi-B Paleomagnetic Locality

[20] About 10 km northeast of the previous paleomagnetic locality, along the road to Longxi, five sites were collected in poorly consolidated brownish red mudstones (Table A7) within a 50-m-thick flat-lying section. This bluff-forming section disconformably overlies strata regionally attributed a Neogene age (Map I-48-IX (Longxi) 1:200,000 [GBGMR, 1989]), suggesting a Pliocene age for the sampled section. Interpretable ChRM directions from all five sites pass the reversals test, and the mean direction is concordant with the expected direction calculated using the Pliocene paleomagnetic pole for Eurasia, likely indicating a primary magnetization (Figure A7).

3.2.6. Heichuan Paleomagnetic Locality

[21] Twelve sites were collected (Table A8) within a folded, 150-m-thick section located at a bridge ~3 km north of the village of Huichuan. On both sides of the river we sampled dark red to purple, well-indurated, fine-grained sandstones and mudstones. Although this part of the section has been broadly grouped with the Lower Cretaceous Hekou Formation (Map 9-48-8 (Lintang), 1:200,000 [GBGMR, 1989]), an Eocene depositional age is indicated by palynomorph assemblages from a gray siltstone collected stratigraphically 150 m upsection above the paleomagnetic locality (sample 02ZX19-P in Table A2 of Horton *et al.* [2004]). At this location we found signs of previous paleomagnetic sampling performed in a smaller part of the section at approximately five sites. We are unaware of any discussion of this paleomagnetic sampling in the literature.

[22] All 12 collected sites yielded interpretable ChRM directions for which pre-folding magnetization is indicated by a positive fold test [McFadden, 1990] (Figure A8). The

locality-mean direction indicates rotation of $22.9 \pm 7.2^\circ$ in a clockwise sense since Eocene time.

3.2.7. Shancheng Paleomagnetic Locality

[23] South of the city of Pingan, a few kilometers north of the village of Shancheng, 17 sites were collected in orange to red fine sandstones to mudstones (Table A9) within a 50-m-thick gently folded sedimentary section forming a bluff along the river. This succession of fluvial sandstone and mudstone interbedded with conglomerate is reported as the lower part of the Upper Cretaceous Minhe Formation conformably above the upper part of the Lower Cretaceous Hekou Formation (Map J-48-121-C (Gaodianzi), 1:50,000 [GBGMR, 1989]). Therefore we consider the section to be of a Late Cretaceous age.

[24] After cleaning of secondary components at lower temperature, 15 of the 17 sites yielded interpretable normal polarity ChRM directions passing the fold test [McFadden, 1990], indicative of pre-folding acquisition of the magnetization (Figure A9 and Table A9). The residual scatter observed in the data after structural correction is attributed to meter-scale intraformational deformation observed on the outcrop.

3.2.8. Gazuan Paleomagnetic Locality

[25] Within the thick sedimentary section located ~10 km south of the city of Pingan, southwest of the village of Gazuan (36°25.09'N; 102°01.33'E), we collected 12 sites in reddish orange beds ranging from matrix-rich medium-grained sandstone to laminated mudstone. These series are stratigraphically within the upper portion of the Late Cretaceous Minhe Formation (Map J-48-121-C (Gaodianzi), 1:50,000 [GBGMR, 1989]). Unfortunately, upon demagnetization of two pilot samples per site, erratic demagnetization behavior and a low intensity of magnetization prevent interpretation of ChRM directions.

3.2.9. East Xining Upper and Lower Paleomagnetic Localities

[26] This section located to the east of the city of Xining was chosen for magnetostratigraphic analysis because of its outstanding continuous exposure of north dipping Upper Jurassic to Eocene fine sandstone and mudstone strata with intercalated gypsum layers. Previous workers have used this section as a standard for regional stratigraphic correlations and provide a basis of palynological analyses (Map J-47-132-B (Xining) 1:50,000 [GBGMR, 1988, 1989; Hao, 1988; Zhai and Cai, 1984]). Our own magnetostratigraphic and biostratigraphic analyses from this and nearby correlatable sections largely corroborate and improve the previous chronostratigraphy [see Horton *et al.*, 2004]. Paleomagnetic results were obtained from the Upper Jurassic to Lower Cretaceous lower part of the section and from the Paleocene-Eocene upper part of the section.

3.2.9.1. Upper Jurassic to Lower Cretaceous Section

[27] In the lower part of the East Xining section (0 to 356 m stratigraphic level), 55 magnetostratigraphic levels were collected from reddish mudstone preferentially sampled over variegated fine- to medium-grained sandstones. The average stratigraphic interval was of ~6 m (Table A10 and Figure A10). Antipodal normal and reverse polarity directions from 46 levels indicate primary magnetization acquired during or shortly after deposition. The reader may consult the companion paper by Horton *et al.* [2004] for magnetostratigraphic analysis of polarity distribution in the

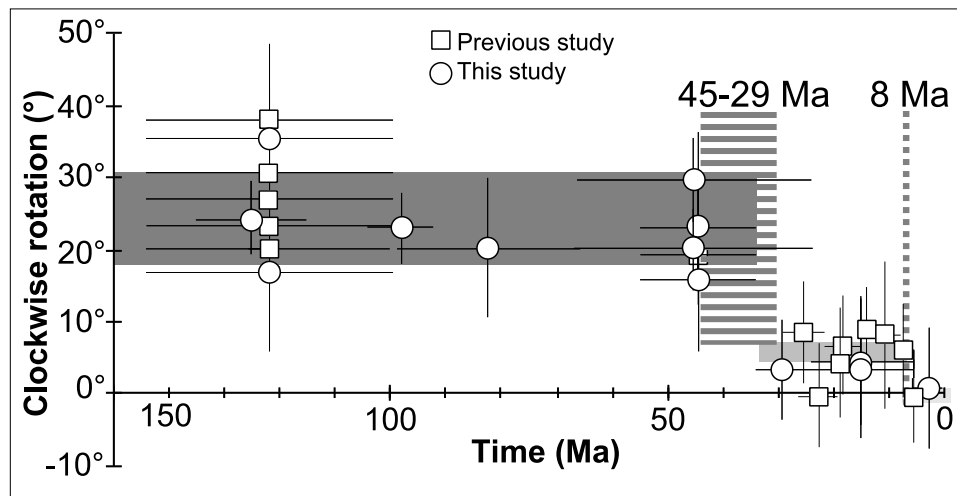


Figure 4. Clockwise rotation relative to the APWP of Eurasia as a function of time since deposition of the sampled rocks (data from Table 1). Thin black lines indicate 95% error bars in clockwise rotation and uncertainty in age. Dashed vertical areas indicated marked step in amount of recorded clockwise rotation and possible age of rotation phases. Shaded areas are arithmetic average of clockwise rotation for the 150–30 Ma ($24.3^\circ \pm 6.5^\circ$), 30–8 Ma ($5.1^\circ \pm 2.8^\circ$), and 8–0 Ma ($-0.2^\circ \pm 1.0^\circ$) periods.

section. For tectonic analysis, 5 to 11 sample ChRM directions from two to three successive levels were gathered to calculate 20 site-mean directions. A positive fold test [McFadden, 1990; McFadden and McElhinny, 1990] on these directions further indicates a primary origin of the magnetization.

3.2.9.2. Paleocene-Eocene Section

[28] In the upper part of the East Xining section (553 to 801 m stratigraphic level), interpretable ChRM directions are obtained from 22 out of 23 magnetostratigraphic levels collected at an average stratigraphic interval of ~ 11 m from almost exclusively gypsum-rich red mudstone. (Table A11 and Figure A11). Primary magnetization is recorded by normal and reverse polarity directions passing the reversals test. The magnetostratigraphic analysis of polarity distribution within the section is developed in the companion paper by Horton *et al.* [2004]. For tectonic analysis, 5–11 sample ChRM directions from two to three successive levels were gathered to calculate nine site-mean directions. Variations in bedding attitudes do not yield a definitive fold test, but a positive reversals test is obtained from the antipodal distribution of normal and reverse polarity directions [McFadden and McElhinny, 1990], indicating primary origin of the magnetization (Figure A11b). Residual scatter of declination in stratigraphic coordinates is attributed to result from bed-parallel slip not identified on the outcrop.

3.2.10. North Xining Paleomagnetic Locality

[29] Directly north of the city of Xining, 18 sites were collected in gypsum-rich red mudstones (Table A12) within a 200-m-thick, gently dipping section of the lower and middle members of the Mahalagou formation (Map J-47-132-B (Xining), 1:50,000 [GBGMR, 1988; Horton *et al.*, 2004; Zhai and Cai, 1984]). Strata from this succession are attributed an early Oligocene age based on fossil assemblages from a nearby section that can be easily correlated using distinctive gypsum marker beds across the Xining region. Interpretable ChRM directions are obtained from all

but one site, and primary origin of the magnetization is confirmed by a positive reversals test.

3.2.11. Xiongshen Paleomagnetic Locality

[30] Within the Hualong basin on the southern flank of the Laji Shan, near the village of Xiongshen, 12 sites were collected in red fine-grained sandstones (Table A13) within a 100-m-thick gently dipping section of the Miocene Xian-shuihe formation (Map J-47-XXXVI (Xining) 1:200,000 [GBGMR, 1989; Horton *et al.*, 2004; Yu *et al.*, 2001]). Out of 12 collected sites, seven yield nearly antipodal ChRM directions of normal and reverse polarity directions suggestive of a primary origin for the magnetization (Figure A13 and Table A13).

4. Discussion

4.1. Results and Implications

[31] Combining our analysis of paleomagnetic declination of primary ChRM obtained from 12 localities with previous results yields a remarkably consistent pattern of vertical axis rotation across the Xining-Lanzhou study region. When compared to the expected declination calculated from the apparent pole wander path (APWP) of Eurasia [Besse and Courtillot, 2002], $19.0 \pm 7.2^\circ$ to $37.8 \pm 10.6^\circ$ clockwise vertical axis tectonic rotations are recorded consistently in all paleomagnetic localities within Eocene and older rocks. In contrast, all paleomagnetic localities within Oligocene to Pliocene rocks have recorded minor to insignificant rotations (Figure 4 and Table 1). Allowing for minor age errors, these results indicate that the Xining-Lanzhou region has undergone a wholesale regional clockwise rotation since late Paleogene time. Using the available age constraints, we can further assess the timescale and the magnitude of the rotational event. The youngest rocks recording the rotation are from the upper section of the East Xining section yielding a middle Eocene age based on chronostratigraphic results presented by

Table 1. Locality Paleomagnetic Directions Compared to Expected Directions in the Xining-Lanzhou Region^a

Locality	Reference	Age	Location		Observed Direction				Reference Pole			Rotation $R \pm \Delta R$, ^b deg	Flattening $F \pm \Delta F$, deg
			Latitude °N	Longitude °E	I , deg	D , deg	α_{95} , deg	Sites n	Latitude °N	Longitude °E	A_{95} , deg		
<i>Xining-Lanzhou Region From This Study</i>													
Longxi B	this study	N ₂	34.97	104.43	56.7	4.8	5.5	5	86.3	172.0	2.6	8.4 ± 0.6	4.8 ± -0.9
Wenfeng	this study	N ₁	34.94	104.80	43.7	8.8	8.5	7	84.2	155.3	1.9	3.1 ± 9.6	14.1 ± 6.9
Xiongshen	this study	N ₁	36.66	101.87	39.2	10.3	8.4	7	84.2	155.3	1.9	4.2 ± 8.9	20.0 ± 6.9
North Xining	this study	E ₃	36.65	101.78	40.2	12.8	5.3	17	82.4	171.7	3.7	3.6 ± 6.7	18.0 ± 5.0
Heichuan	this study	E ₂	35.16	103.97	51.5	32.8	5.4	12	80.9	160.8	1.8	22.9 ± 7.2	7.5 ± 4.5
Shancheng	this study	K ₂	36.38	102.05	33.9	30.1	9.6	15	81.3	206.6	2.4	20.0 ± 9.6	19.3 ± 7.9
Longxi A	this study	K ₁	34.93	104.39	40.1	47.7	6.2	6	79.8	188.0	2.5	35.2 ± 6.9	14.8 ± 5.3
East Xining upper	this study	E ₂	36.58	101.89	33.7	26.8	11.9	9	80.9	160.8	1.8	16.5 ± 11.6	26.3 ± 9.6
East Xining lower	this study	K ₁	36.58	101.89	33.6	37.7	4.5	20	79.8	188.0	2.5	25.1 ± 5.0	22.3 ± 4.1
Danchang basin													
Niuding Shan	this study	E	34.18	104.81	55.3	28.5	3.1	7	81.6	162.5	1.4	19.4 ± 4.6	2.4 ± 2.7
Nanyang	this study	E	33.97	104.67	57.6	38.1	3.0	4	81.6	162.5	1.4	29.1 ± 4.7	-0.1 ± 2.6
Dangchang	this study	K ₁	34.08	104.47	50.9	35.8	2.9	18	79.8	188.0	2.5	23.5 ± 4.4	3.1 ± 3.1
<i>Xining-Lanzhou Region From Previous Studies</i>													
Linxia HWJ ^c	<i>Fang et al.</i> [2003]	5	35.70	103.10	40	3.4	5.7	67 m	86.3	172.0	2.6	-0.9 ± 6.5	16.4 ± 5.0
Linxia LS ^c	<i>Fang et al.</i> [2003]	5	35.70	103.10	34.5	9.9	6.1	51 m	86.3	172.0	2.6	5.6 ± 6.5	21.9 ± 5.3
Linxia DX ^c	<i>Fang et al.</i> [2003]	10	35.70	103.10	43	13.7	4.6	84 m	85.0	155.7	3.1	8.6 ± 6.0	15.0 ± 4.3
Linxia SZ ^c	<i>Fang et al.</i> [2003]	15	35.70	103.10	33.4	13.7	10.1	41 m	84.2	154.9	3.2	7.8 ± 10.2	25.0 ± 8.4
Linxia ZZ ^c	<i>Fang et al.</i> [2003]	20	35.70	103.10	39.5	14.6	5	84 m	81.4	149.7	4.5	6.3 ± 7.1	20.9 ± 5.1
Linxia TL ^c	<i>Fang et al.</i> [2003]	25	35.70	103.10	37.2	14.3	4.7	91 m	83.8	153.2	5.3	8.1 ± 7.2	21.6 ± 5.4
Duitingou	<i>Flynn et al.</i> [1999]	20	36.23	103.23	38.2	8	4.7	100 m	81.4	149.7	4.5	-0.4 ± 6.8	22.6 ± 4.9
Duitingou	<i>Flynn et al.</i> [1999]	25	36.23	103.23	37.8	10	4.7	55 m	83.8	153.2	5.3	3.8 ± 7.3	21.5 ± 5.3
Honggoou Formation	<i>Cogne et al.</i> [1999]	E ₂	36.50	102.00	40.8	29.3	13.2	5	80.9	160.8	1.8	19.0 ± 14.2	19.1 ± 10.6
Ryuieshan	<i>Halim et al.</i> [1998]	K ₁	36.50	101.15	37.8	35.8	6.3	1	79.8	188.0	2.5	23.1 ± 6.9	18.0 ± 5.4
Minhe	<i>Halim et al.</i> [1998]	K ₁	36.30	102.90	40.4	50.5	9.8	3	79.8	188.0	2.5	37.8 ± 10.6	15.6 ± 8.1
Lanzhou	<i>Halim et al.</i> [1998]	K ₁	36.20	103.40	46.9	43.2	6.8	6	79.8	188.0	2.5	30.5 ± 8.4	9.0 ± 5.8
Lintao A	<i>Yang et al.</i> [2002]	K ₁	35.85	103.78	50.3	32.3	4.2	11	79.8	188.0	2.5	19.7 ± 5.8	5.4 ± 3.9
Lintao B	<i>Yang et al.</i> [2002]	K ₁	35.83	103.77	48.9	39.3	7.5	4	79.8	188.0	2.5	26.7 ± 9.5	6.8 ± 6.3
Dingxi	<i>Yang et al.</i> [2002]	K ₁	35.57	104.31	51.4	29.2	8.3	4	79.8	188.0	2.5	16.6 ± 11.0	4.1 ± 6.9

^aSee Figure 2. Locality is name of paleomagnetic sampling locality; age is geological age of sampled formations: J₃, Late Jurassic; K₁, Early Cretaceous; K₂, Late Cretaceous; E₁, Paleocene; E₂, Eocene; E₃, Oligocene; N₁, Miocene; N₂, Pliocene. Latitude and longitude are of sampling locality. Observed direction is mean paleomagnetic direction: I and D are inclination and declination in stratigraphic coordinates with α_{95} the radius of 95% confidence circle. Site n is number of sites used to calculate mean direction ("m" indicates that magnetostratigraphic levels are included). For the reference pole, latitude and longitude, and A_{95} , the 95% confidence limit of Eurasian paleomagnetic pole, [Besse and Courtillot, 2002] are calculated using the following age windows: J₃, 135–155 Ma; K₁, 95–135 Ma; K₂, 65–95 Ma; E₁, 55–65 Ma; E₂, 35–55 Ma; E₃, 25–35 Ma; N₁, 5–25 Ma; N₂, 5 Ma. Rotation $R \pm \Delta R$ is the vertical axis rotation with 95% confidence limit (positive indicates clockwise rotation). Flattening $F \pm \Delta F$ is the flattening of inclination with 95% confidence limit. Rotation and flattening are derived from observed direction minus expected direction at locality calculated from reference pole.

^bArithmetic averages of rotation with standard deviation are 24.3 ± 6.5 for results older than Oligocene, 5.1 ± 2.8 for results from 29 to 8 Ma, and -0.2 ± 1.0 for results younger than 8 Ma.

^cLocality abbreviations are from *Fang et al.* [2003].

Horton et al. [2004]. Arguably, the smaller $16.5 \pm 11.6^\circ$ clockwise rotations observed in these rocks may indicate deposition during the rotation. The oldest rocks that have not suffered from significant rotation are the sediments of the Linxia basin, yielding magnetostratigraphic ages of 1.7–29 Ma [Fang et al., 2003]. Close inspection of the Linxia basin results may indicate small clockwise rotation occurring at circa 8 Ma. The sum of these constraints suggests that most of the rotation (arithmetic mean $24.3 \pm 6.5^\circ$) occurred during a major phase of rotation that started as early as mid-Eocene (circa 45 Ma) and ended before 29 Ma. This event is possibly followed by minor rotation (arithmetic mean $5.1^\circ \pm 2.6^\circ$) during a secondary late Miocene phase. While the minor late Miocene phase of rotation can be easily correlated to the regional Miocene tectonic events recorded in sedimentary and thermochronological studies [Kirby et al., 2002; Metivier et al., 1998; Meyer et al., 1998], the timing of the main late Paleogene rotation phase underscores the existence of an important early tectonic event in northern part of the present-day Tibetan Plateau.

[32] The timing of this tectonic event is in good agreement with our chronostratigraphic analysis of the northeastern Tibetan Plateau indicating a doubling of accumulation rates during Paleogene time [Horton et al., 2004]. In addition, ~ 30 Ma exhumation ages are obtained in the nearby Kunlun range [Mock et al., 1999], while a regional study based on apatite fission track analysis around the margins of the Qaidam basin, within the entire Nan Shan fold thrust belt, the Altyn Shan and the Kunlun belt indicate a general increased exhumation rate at ~ 40 and ~ 10 Ma [Jolivet et al., 2002]. Confirming the trend previously suggested by these studies, important tectonic rotations in northeastern Tibet during Eocene time indicates that significant deformation reached this region shortly after the initial collision of India with Asia rather than during Miocene to Pliocene time after slow northward propagation of deformation [Metivier et al., 1998; Meyer et al., 1998; Tapponnier et al., 2001].

4.2. Regional Extent and Mechanism for the Rotation

[33] To understand and identify possible mechanisms responsible for the rotation of the study area, we compiled

all rotational information provided by Jurassic to Tertiary paleomagnetic results surrounding the Xining-Lanzhou area (Table A14 and Figure 1). This, in turn, is used to assess whether the Eocene rotations recorded in the Xining-Lanzhou region match rotations of surrounding regions.

[34] To the north and east of the study area, no significant tectonic rotations are recorded in Middle Jurassic to Tertiary red beds of the North China block [Ma *et al.*, 1993], the Ordos basin [Yang *et al.*, 1992], and along the Hexi corridor [Chen *et al.*, 2002b; Dupont-Nivet *et al.*, 2003]. This indicates the existence of a major tectonic boundary to accommodate the Eocene clockwise rotation between these regions and the Xining-Lanzhou region. Obvious candidates for this boundary are the left-lateral Haiyuan fault and Liupan Shan restraining bend. However, these structures have been recognized to accommodate limited Miocene to Pliocene displacement [Burchfiel *et al.*, 1991; Gaudemer *et al.*, 1995; Lasserre *et al.*, 2002]. Identification of remnant Paleogene structures is impaired by subsequent sedimentation and thrusting related to Neogene deformation in this region; however, paleomagnetic results reveal that unrecognized structures or the Haiyuan fault may have been active during Eocene time to accommodate the rotation of the study area.

[35] To the south of the Xining-Lanzhou region, clockwise rotations are reported from the eastern Tibetan Plateau within the Songpan-Ganzi and Qiangtang terranes [Cogné *et al.*, 1999; Halim *et al.*, 1998; Huang *et al.*, 1992; Lin and Watts, 1988; Otofujii *et al.*, 1990], in contrast with the absence of significant rotations in the South China block to the east [Enkin *et al.*, 1991; Yokoyama *et al.*, 2001, 1999] and in the Lhasa terrane to the west [Lin and Watts, 1988] (Figure 1). A pattern of clockwise rotation increasing toward the eastern margin of the Tibetan Plateau is interpreted to result from either right-lateral shear in response to the indentation of India into Asia [Cobbold and Davy, 1988; Dewey *et al.*, 1988; England and Houseman, 1985; England and Molnar, 1990] or eastward rotational extrusion along curved left-lateral faults [Molnar and Lyon-Caen, 1989; Peltzer and Tapponnier, 1988]. Most of the eastern Tibetan paleomagnetic data set has been collected preferentially in Cretaceous strata suitable for paleomagnetic studies, such that the timing of rotation can only be constrained to be broadly post-Cretaceous. Our results suggest that the regional tectonic process involving clockwise rotation extended along the eastern margin of the Tibetan Plateau as far north as the Xining-Lanzhou region during late Paleogene time. The subsequent extrusion of Indochina at 35–17 Ma [Leloup *et al.*, 1995; Sato *et al.*, 2001] and possible activation of the Altyn Tagh fault [Bally *et al.*, 1986; Ritts *et al.*, 2001] mark the beginning of a tectonic setting that may correlate with the end of the rotation phase at the eastern margin of the Himalaya-Tibetan orogen. Further paleomagnetic results from well-dated Tertiary rocks of the eastern Tibetan Plateau are needed to test these hypotheses.

[36] To the west of the study area, in the Qaidam basin and the Nan Shan fold-thrust belt, paleomagnetic results from sedimentary rocks of Oligocene and younger age indicate no rotations of these regions since Oligocene time (see Dupont-Nivet *et al.* [2003] for a review). Scarce data from poorly dated older strata are inconclusive with regard

to the pre-Oligocene rotational history of these regions [Chen *et al.*, 2002a; Frost *et al.*, 1995]. In considering whether or not the Eocene clockwise rotation of northeastern Tibet extended into the Qaidam basin and Nan Shan fold-thrust belt, at least two possible mechanisms can be considered: model A, wholesale clockwise rotation of the Qaidam basin, Nan Shan fold-thrust belt, and Xining-Lanzhou area through rotational extrusion along the Altyn Tagh fault, similar to the proposal of [Chen *et al.*, 2002a], but during late Paleogene time (Figure 5a); or model B, clockwise rotation of a crustal fragment including the Xining-Lanzhou region, through right-lateral shear on the eastern margin of the Qaidam basin, with the Qaidam block acting as a secondary indenter [Dupont-Nivet *et al.*, 2002] (Figure 5b). Through model A, a 25° rotation of the area between the Xining-Lanzhou and Qaidam regions would require 600 km of pre-Oligocene left-lateral offset on the Altyn Tagh fault (assuming the Euler pole of rotation of Chen *et al.* [2002a]) and accommodation of 600 km of eastward extrusion in the South China block. These large-magnitude displacements are incompatible with current kinematic constraints on Tertiary deformation. Estimates of left-lateral slip along the Altyn Tagh fault range from 700 to 60 km [Tapponnier *et al.*, 1981; Wang, 1997], but recent studies constrain the offset to 375 ± 25 km [Gehrels *et al.*, 2003; Meng *et al.*, 2001; Ritts and Biffi, 2000; Ritts *et al.*, 2004; Yin and Harrison, 2000; Yue *et al.*, 2001, 2004]. These studies suggest Oligocene piercing points showing the same (or nearly the same) offset as pre-Tertiary piercing points, ruling out pre-Oligocene slip on the fault required by model A. Likewise, the maximum 100 km shortening in the Longmen Shan [Burchfiel *et al.*, 1995] and the absence of pre-Oligocene major strike-slip faults or tectonic rotation east of the northeastern Tibetan Plateau cannot accommodate the 600 km eastward extrusion required by model A. In model B, 25° clockwise rotation of a 400-km-wide crustal fragment limited to the north by the left-lateral Haiyuan fault and to the west the right-lateral Haiyuan fault would require a maximum differential convergence of 170 km between the Qaidam indenter and the North China block. We argue that this convergence may have been accommodated by late Eocene shortening within the Nan Shan fold-thrust [Bally *et al.*, 1986; A. C. Robinson *et al.*, 2002; Yin *et al.*, 2002]. This mechanism does not exclude the possibility that some of the rotation has been accommodated partially through left lateral motion on the Haiyuan and related faults and early extension in the Ordos basin [Zhang *et al.*, 1998]. Because model A requires drastic tectonic implications and violates constraints imposed by the amount and timing of offset on the Altyn Tagh fault, we prefer model B to explain the rotation of the Xining-Lanzhou region. These end-member mechanisms can be further tested by assessing tectonic rotations through paleomagnetic analysis of Tertiary sedimentary rocks in the Qaidam basin and Nan Shan fold-thrust belt and within the eastern margin of the Tibetan Plateau.

5. Conclusion

[37] Paleomagnetic results obtained from 127 sites at 12 localities yield primary magnetizations confirmed by fold, reversal, and conglomerate tests within the Xining-

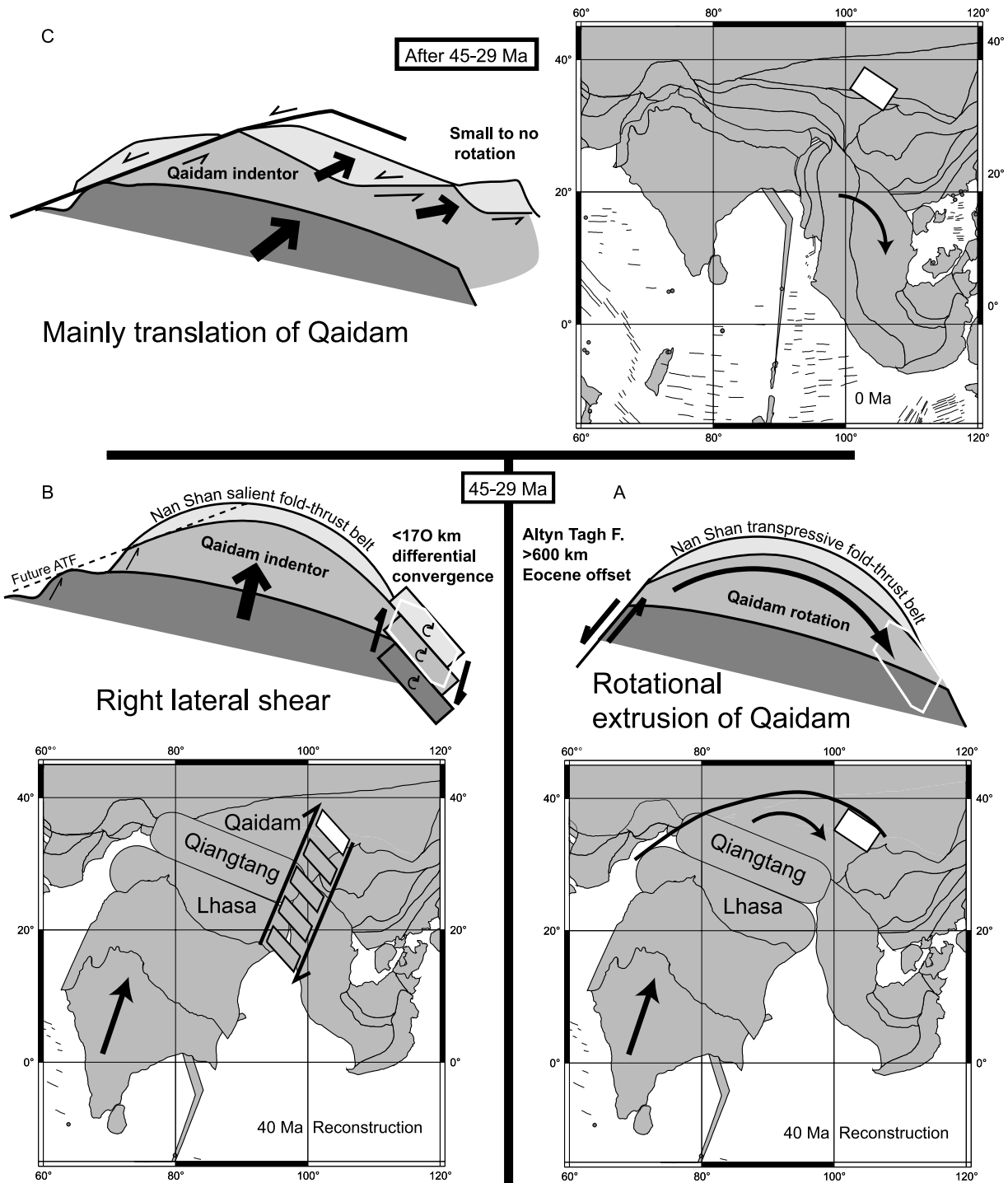


Figure 5. Tectonic mechanisms. (a) Early eastward rotational extrusion along proto-left-lateral Altyn Tagh fault to the north drives $\sim 25^\circ$ rotation of the Qaidam, the Nan Shan fold-thrust belt, and the Xining-Lanzhou region. (b) Right-lateral shear corridor extending on the eastern margin of the Himalaya-Tibetan orogen drives $\sim 25^\circ$ clockwise rotation of the Xining-Lanzhou region. (c) After the end of main rotation phase Qaidam Basin translates without rotation along the Altyn Tagh Fault, which drives crustal thickening in the Nan Shan fold-thrust belt.

Lanzhou region in the northeastern Tibetan Plateau. Age control on the collected rocks is provided by a regional chronostratigraphic synthesis presented in the companion paper by *Horton et al.* [2004]. Combining our results with

paleomagnetic declinations from previous studies indicates that the Xining-Lanzhou region has undergone a wholesale regional clockwise rotation during late Paleogene time. We can establish that most of the rotation (arithmetic mean

$24.3 \pm 6.5^\circ$) occurred during a major phase of rotation that started as early as mid-Eocene (circa 45 Ma) and ended before 29 Ma. This event was possibly followed by minor rotation (arithmetic mean: $5.1^\circ \pm 2.6^\circ$) during a secondary late Miocene phase. The minor late Miocene phase of rotation can be easily correlated to the regional Miocene tectonic events recorded in sedimentary and thermochronological studies [Kirby *et al.*, 2002; Metivier *et al.*, 1998; Meyer *et al.*, 1998]. The timing of the major late Paleogene rotation phase is consistent with regional sedimentary [Horton *et al.*, 2004] and thermochronologic constraints [Jolivet *et al.*, 2002; Mock *et al.*, 1999]. This underscores the existence of an important early tectonic event reaching regions of the northern Tibetan Plateau shortly after the initial collision of India with Asia. Using a compilation of paleomagnetic data over the eastern Tibetan Plateau and based on consistency with geologic data, the clockwise rotation of the Xining-Lanzhou region is explained through right-lateral shear, and associated shortening, in response to northward indentation of the Qaidam basin.

[38] **Acknowledgments.** This work was funded by grant PRF-37207-G8 (Horton) from the American Chemical Society (Petroleum Research Fund), grant EAR-0106677 (Horton) from the National Science Foundation, and a Geological Society of America research grant (Dupont-Nivet). We thank Jianghai Wang, Huihua Zhang, and Xiaowei Jiang (Chinese Academy of Sciences, Institute of Geochemistry, Guangzhou) for logistical and field assistance. Part of the paleomagnetic analysis was performed using software by R. K. Enkin. We are grateful to Brad Ritts, Associate Editor R. K. Enkin, and an anonymous reviewer for constructive comments.

References

- Argand, E. (1924), La tectonique de l'Asie, *Int. Geol. Cong. Session Rep.*, 13, 170–372.
- Bally, A. W., I. M. Chou, R. Clayton, H. P. Eugster, S. Kidwell, L. D. Meckel, R. T. Ryder, A. B. Watts, and A. A. Wilson (1986), Notes on sedimentary basins in China: Report of the American Sedimentary Basins Delegation to the People's Republic of China, *U.S. Geol. Surv. Open File Rep.*, 86–237, 108 pp.
- Beck, M. E. (1980), Paleomagnetic record of plate-margin tectonic processes along the western edge of North America, *J. Geophys. Res.*, 85(B12), 7115–7131.
- Bendick, R., R. Bilham, J. Freymueller, K. Larson, and G. Yin (2000), Geodetic evidence for a low slip rate in the Altyn Tagh fault system, *Nature*, 404, 69–72.
- Besse, J., and V. Courtillot (1988), Paleogeographic maps of the continents bordering the Indian Ocean since the Early Jurassic, *J. Geophys. Res.*, 93(B10), 11,791–11,808.
- Besse, J., and V. Courtillot (2002), Apparent and true polar wander and the geometry of the geomagnetic field in the last 200 million years, *J. Geophys. Res.*, 107(B11), 2300, doi:10.1029/2000JB000050.
- Burbank, D. W., R. A. Beck, and T. Mulder (1996), The Himalayan foreland basin, in *Tectonic Evolution of Asia, Rubey Volume IX*, edited by A. Yin and T. M. Harrison, pp. 149–189, Cambridge Univ. Press, New York.
- Burchfiel, B. C., Z. Peizhen, W. Yipeng, Z. Weiqi, S. Fangmin, D. Qidong, P. Molnar, and L. Royden (1991), Geology of the Haiyuan fault zone, Ningxia-hui autonomous region, China, and its relation to the evolution of the northeastern margin of the Tibetan Plateau, *Tectonics*, 10(6), 1091–1110.
- Burchfiel, B. C., Z. Chen, Y. Liu, and L. H. Royden (1995), Tectonics of the Longmen Shan and adjacent regions, central China, *Int. Geol. Rev.*, 37(8), 661–735.
- Butler, R. F. (1992), *Paleomagnetism: Magnetic Domains to Geologic Terranes*, pp. 83–104, Blackwell Sci., Malden, Mass.
- Chen, Y., S. Gilder, N. Halim, J.-P. Cogné, and V. Courtillot (2002a), New Mesozoic and Cenozoic paleomagnetic data help constrain the age of motion on the Altyn Tagh fault and rotation of the Qaidam basin, *Tectonics*, 21(5), 1042, doi:10.1029/2001TC901030.
- Chen, Y., H. Wu, V. Courtillot, and S. Gilder (2002b), Large N-S convergence at the northern edge of the Tibetan Plateau? New Early Cretaceous paleomagnetic data from the Hexi Corridor, NW China, *Earth Planet. Sci. Lett.*, 201, 293–307.
- Chen, Z., B. C. Burchfiel, Y. Liu, R. W. King, L. H. Royden, W. Tang, E. Wang, J. Zhao, and X. Zhang (2000), Global Positioning System measurements from eastern Tibet and their implications for India/Eurasia intercontinental deformation, *J. Geophys. Res.*, 105(B7), 16,215–16,227.
- Cobbold, P. R., and P. Davy (1988), Indentation tectonics in nature and experiments, 2. central Asia, *Bull. Geol. Inst. Uppsala*, 14, 143–162.
- Cogné, J. P., N. Halim, Y. Chen, and V. Courtillot (1999), Resolving the problem of shallow magnetizations of Tertiary age in Asia: Insights from paleomagnetic data from the Qiangtang, Kunlun, and Qaidam blocks (Tibet, China), and a new hypothesis, *J. Geophys. Res.*, 104(B8), 17,715–17,734.
- DeCelles, P. G., G. E. Gehrels, Q. J., O. T. P., and P. A. Kapp (1998), Neogen foreland basin deposits, erosional unroofing, and the kinematic history of the Himalayan fold-thrust belt, western Nepal, *Geol. Soc. Am. Bull.*, 110, 2–21.
- DeCelles, P. G., D. M. Robinson, and G. Zandt (2002), Implications of shortening in the Himalayan fold-thrust belt for uplift of the Tibetan Plateau, *Tectonics*, 21(6), 1062, doi:10.1029/2001TC001322.
- Demarest, H. H. (1983), Error analysis of the determination of tectonic rotations from paleomagnetic data, *J. Geophys. Res.*, 88, 4321–4328.
- Dewey, J. F., R. M. Shackleton, C. Chengfa, and S. Yiyin (1988), The tectonic evolution of the Tibetan Plateau, *Philos. Trans. R. Soc. London*, 327, 379–413.
- Ding, Z. L., S. L. Yang, J. M. Sun, and T. S. Liu (2001), Iron geochemistry of loess and red clay deposits in the Chinese Loess Plateau and implications for long-term Asian monsoon evolution in the last 7.0 Ma, *Earth Planet. Sci. Lett.*, 185, 99–109.
- Dupont-Nivet, G., R. F. Butler, A. Yin, and X. Chen (2002), Paleomagnetism indicates no Neogene rotation of the Qaidam basin in north Tibet during Indo-Asian collision, *Geology*, 30(3), 263–266.
- Dupont-Nivet, G., R. F. Butler, A. Yin, and X. Chen (2003), Paleomagnetism indicates no Neogene rotation of the Northeastern Tibetan Plateau, *J. Geophys. Res.*, 108(B8), 2386, doi:10.1029/2003JB002399.
- England, P., and G. Houseman (1985), Role of lithospheric strength heterogeneities in the tectonics of Tibet and neighbouring regions, *Nature*, 315, 297–301.
- England, P. C., and G. A. Houseman (1988), The mechanics of the Tibetan Plateau, *Philos. Trans. R. Soc. London*, 326, 301–320.
- England, P., and P. Molnar (1990), Right-lateral shear and rotation as the explanation for strike-slip faulting in eastern Tibet, *Nature*, 344, 140–142.
- England, P., and P. Molnar (1997), The field of crustal velocity in Asia calculated from Quaternary rates of slip on faults, *Geophys. J. Int.*, 130, 551–582.
- Enkin, R. J., Y. Chen, V. Courtillot, J. Besse, L. Xing, Z. Zhang, Z. Zhuang, and J. Zhang (1991), A Cretaceous pole from south China, and the Mesozoic hairpin turn of the Eurasian apparent polar wander path, *J. Geophys. Res.*, 96, 4007–4027.
- Fang, X., C. Garzzone, R. Van der Voo, J. Li, and M. Fan (2003), Flexural subsidence by 29 Ma on the NE edge of Tibet from the magnetostratigraphy of Linxia basin, China, *Earth Planet. Sci. Lett.*, 210(3–4), 545–560.
- Fisher, R. A. (1953), Dispersion on a sphere, *Proc. R. Soc. London, Ser. A*, 217, 295–305.
- Flynn, L. J., W. Downs, N. D. Opdyke, K. Huang, E. Lindsay, J. Ye, G. Xie, and X. Wang (1999), Recent advances in the small mammal biostratigraphy and magnetostratigraphy of Lanzhou basin, *Chin. Sci. Bull.*, 44, Suppl., 109–117.
- Frost, G. M., R. S. Coe, Z. Meng, Z. Peng, Y. Chen, V. Courtillot, G. Peltzer, P. Tapponnier, and J. P. Avouac (1995), Preliminary early Cretaceous paleomagnetic results from the Gansu Corridor, China, *Earth Planet. Sci. Lett.*, 129, 217–232.
- Gansu Bureau of Geology and Mineral Resources (GBGMR) (1988), Geologic maps of the Daheba, Dangchang, Lianggongzhen, and Xinhua regions (4 sheets), with regional geologic report (1:50,000 scale), 120 pp., Lanzhou, China.
- Gansu Bureau of Geology and Mineral Resources (GBGMR) (1989), *Regional Geology of Gansu Province* (in Chinese with English summary), 690 pp., Geol. Publ. House, Beijing.
- Gaudemer, Y., P. Tapponnier, B. Meyer, G. Peltzer, G. Shummin, Z. Chen, H. Dai, and I. Cifuentes (1995), Partitioning of crustal slip between linked, active faults in the eastern Qilian Shan and evidence for major seismic gap, the “Tianzu gap,” on the western Haiyuan Fault, Gansu (China), *Geophys. J. Int.*, 120, 599–645.
- Gehrels, G. E., A. Yin, and X. Wang (2003), Detrital-zircon geochronology of the northeastern Tibetan Plateau, *Geol. Soc. Am. Bull.*, 115, 881–896.
- Halim, N., J. P. Cogné, Y. Chen, R. Atasesi, J. Besse, V. Courtillot, S. Gilder, J. Marcoux, and R. L. Zhao (1998), New Cretaceous and early Tertiary paleomagnetic results from Xining-Lanzhou basin, Kunlun and Qiangtang blocks, China: Implications on the geodynamic evolution of Asia, *J. Geophys. Res.*, 103(B9), 21,025–21,045.

- Hao, Y. C. (1988), Cretaceous and Palaeogene ostracod biostratigraphy in Xining and Minhe basins of China, in *Evolutionary Biology of Ostracoda*, edited by T. Hanai, N. Ikeya, and K. Ishizaki, pp. 1163–1171, Elsevier Sci., New York.
- Holt, W. E., and A. J. Haines (1993), Velocity fields in deforming Asia from the inversion of earthquake-released strains, *Tectonics*, *12*(1), 1–20.
- Holt, W. E., N. Chamot-Rooke, X. Le Pichon, A. J. Haines, B. Shen-Tu, and J. Ren (2000), Velocity field in Asia inferred from Quaternary fault slip rates and Global Positioning System observations, *J. Geophys. Res.*, *105*(B8), 19,185–19,209.
- Horton, B. K., A. Yin, M. S. Spurlin, J. Zhou, and J. Wang (2002), Paleocene-Eocene syncontractual sedimentation in narrow, lacustrine-dominated basins of east-central Tibet, *Geol. Soc. Am. Bull.*, *114*, 771–786.
- Horton, B. K., G. Dupont-Nivet, J. Zhou, G. L. Waanders, R. F. Butler, and J. Wang (2004), Mesozoic-Cenozoic evolution of the Xining-Minhe and Dangchang basins, northeastern Tibetan Plateau: Magnetostratigraphic and biostratigraphic results, *J. Geophys. Res.*, *109*, B04402, doi:10.1029/2003JB002913.
- Huang, K., N. D. Opdyke, J. Li, and X. Peng (1992), Paleomagnetism of Cretaceous rocks from eastern Qiangtang terrane of Tibet, *J. Geophys. Res.*, *97*(B2), 1789–1799.
- Jolivet, M., M. Brunel, D. Seward, Z. Xu, J. Yang, F. Roger, P. Tapponnier, J. Malavieille, N. Arnaud, and C. Wu (2002), Mesozoic and Cenozoic tectonics of the northern edge of the Tibetan Plateau: Fission-track constraints, *Tectonophysics*, *343*(1–2), 111–134.
- Kirby, E., P. W. Reiners, M. A. Krol, K. X. Whipple, K. V. Hodges, K. A. Farley, W. Tang, and Z. Chen (2002), Late Cenozoic evolution of the eastern margin of the Tibetan Plateau: Inferences from $^{40}\text{Ar}/^{39}\text{Ar}$ and (U-Th)/He thermochronology, *Tectonics*, *21*(1), 1001, doi:10.1029/2000TC001246.
- Kirschvink, J. L. (1980), The least-square line and plane and the analysis of paleomagnetic data, *Geophys. J. R. Astron. Soc.*, *62*, 699–718.
- Klootwijk, C. T., P. J. Conaghan, and C. M. Powell (1985), The Himalayan Arc: Large-scale continental subduction, oroclinal bending and back-arc spreading, *Earth Planet. Sci. Lett.*, *75*, 167–183.
- Lasserre, C., Y. Gaudemer, P. Tapponnier, A. S. Mériaux, J. van der Woerd, Y. Daoyang, R. F. J., R. Finkel, and M. Caffee (2002), Fast late Pleistocene slip rate on the Leng Long Ling segment of the Haiyuan fault, Qinghai, China, *J. Geophys. Res.*, *107*(B11), 2276, doi:10.1029/2000JB000060.
- Leloup, P. H., R. Lacassin, P. Tapponnier, U. Scharer, Z. Dalai, X. H. Liu, J. S. Zhang, S. C. Ji, and P. T. Trinh (1995), The Ailao Shan-Red River shear zone (Yunnan, China), Tertiary transform boundary of Indochina, *Tectonophysics*, *251*, 3–84.
- Le Pichon, X., M. Fournier, and L. Jolivet (1992), Kinematics, topography, shortening, and extrusion in the India-Eurasia collision, *Tectonics*, *11*(6), 1085–1098.
- Lin, J., and D. R. Watts (1988), Paleomagnetic results from the Tibetan Plateau, *Philos. Trans. R. Soc. London*, *327*, 239–262.
- Liu, T., M. Ding, and E. Derbyshire (1998), Gravel deposits on the margin of the Qinghai-Xizang Plateau, and their environmental significance, *Palaeogeogr. Palaeoclimatol. Palaeoecol.*, *120*, 159–170.
- Ma, X., Z. Yang, and L. Xing (1993), The Lower Cretaceous reference pole for north China and its tectonic implications, *Geophys. J. Int.*, *115*, 323–331.
- Mattauer, M., P. Matte, and J.-L. Olivet (1999), A 3D model of the India-Asia collision at plate scale, *C. R. Acad. Sci., Ser. IIA*, *328*(8), 499–508.
- McFadden, P. L. (1990), A new fold test for palaeomagnetic studies, *Geophys. J. Int.*, *103*, 163–169.
- McFadden, P. L., and M. W. McElhinny (1990), Classification of the reversal test in palaeomagnetism, *Geophys. J. Int.*, *103*, 725–729.
- Meng, Q.-R., J.-M. Hu, and F.-Z. Yang (2001), Timing and magnitude of displacement on the Altyn Tagh fault: Constraints from stratigraphic correlation of adjoining Tarim and Qaidam basins, NW China, *Terra Nova*, *13*(2), 86–91.
- Metivier, F., Y. Gaudemer, P. Tapponnier, and B. Meyer (1998), North-eastward growth of the Tibet plateau deduced from balanced reconstruction of two depositional areas: The Qaidam and Hexi corridor basins, China, *Tectonics*, *17*(6), 823–842.
- Meyer, B., P. Tapponnier, L. Bourjot, F. Metivier, Y. Gaudemer, G. Peltzer, G. Shummin, and C. Zhitai (1998), Crustal thickening in the Gansu-Qinghai, lithospheric mantle, oblique and strike-slip controlled growth of the Tibetan Plateau, *Geophys. J. Int.*, *135*, 1–47.
- Mock, C., N. Arnaud, and J.-M. Cantagrel (1999), An early unroofing in northeastern Tibet? Constraints from $^{40}\text{Ar}/^{39}\text{Ar}$ thermochronology on granitoids from the eastern Kunlun range (Qinghai, NW China), *Earth Planet. Sci. Lett.*, *171*, 107–122.
- Molnar, P., and H. Lyon-Caen (1989), Fault plane solutions of earthquakes and active tectonics of the Tibetan Plateau and its margins, *Geophys. J. Int.*, *99*, 123–153.
- Molnar, P., and P. Tapponnier (1975), Cenozoic tectonics of Asia: Effects of a continental collision, *Science*, *189*, 419–426.
- Molnar, P., P. England, and J. Martinod (1993), Mantle dynamics, uplift of the Tibetan Plateau, and the Indian monsoon, *Rev. Geophys.*, *31*(4), 357–396.
- Otofujii, Y., S. Inoue, S. Funahara, F. Murata, and X. Zheng (1990), Palaeomagnetic study of eastern Tibet-deformation of the Three Rivers region, *Geophys. J. Int.*, *103*, 85–94.
- Peltzer, G., and F. Saucier (1996), Present-day kinematics of Asia derived from geologic fault rates, *J. Geophys. Res.*, *101*(B12), 27,943–27,956.
- Peltzer, G., and P. Tapponnier (1988), Formation and evolution of strike-slip faults, rifts, and basins during the India-Asia collision: An experimental approach, *J. Geophys. Res.*, *93*(B12), 15,085–15,117.
- Peltzer, G., P. Tapponnier, and R. Armijo (1989), Magnitude of late Quaternary, left-lateral movement along the north edge of Tibet, *Science*, *246*, 1285–1289.
- Qinghai Bureau of Geology and Mineral Resources (QBGM) (1985), Geologic maps of the Duoba, Gaodian, Tianjiazai, and Xining regions (4 sheets), with regional geologic report (1:50,000 scale), 199 pp., Xining, China.
- Qinghai Bureau of Geology and Mineral Resources (QBGM) (1991), *Regional Geology of the Qinghai Province*, 662 pp., Geol. Publ. House, Beijing.
- Ratschbacher, L., W. Frisch, C. Chen, and G. Pan (1996), Cenozoic deformation, rotation, and stress patterns in eastern Tibet and western Sichuan, China, in *Tectonic Evolution of Asia, Rubey Volume IX*, edited by A. Yin and T. M. Harrison, pp. 227–249, Cambridge Univ. Press, New York.
- Ritts, B. D., and U. Biffi (2000), Magnitude of post-Middle Jurassic (Bajocian) displacement on the central Altyn Tagh fault system, northwest China, *Geol. Soc. Am. Bull.*, *112*, 61–74.
- Ritts, B. D., and U. Biffi (2001), Mesozoic northeast Qaidam basin: Response to contractional reactivation of the Qilian Shan, and implications for the extent of Mesozoic intracontinental deformation in central Asia, in *Paleozoic and Mesozoic Tectonic Evolution of Central Asia: From Continental Assembly to Intracontinental Deformation*, edited by S. H. Marc and A. D. Gregory, Geol. Soc. of Am., Boulder, Colo.
- Ritts, B. D., B. J. Darby, and T. Cope (2001), Early Jurassic extensional basin formation in the Daqing Shan segment of the Yinshan Belt, northern North China block, Inner Mongolia, *Tectonophysics*, *339*(3–4), 239–258.
- Ritts, B. D., Y. Yue, and S. A. Graham (2004), Oligo-Miocene tectonics and sedimentation along the Altyn Tagh fault, northern Tibetan Plateau: Analysis of the Xorkol, Subei, Aksai basins, *J. Geol.*, in press.
- Robinson, A. C., A. Yin, C. A. Menold, X. Chen, and W. X. Feng (2002), Tertiary Shortening along the Eastern Portion of the North Qaidam Thrust System, *Eos Trans. AGU*, *83*(47), Abstract T51B-1158.
- Robinson, D. M., G. Dupont-Nivet, G. E. Gehrels, and Y. Zhang (2002), The Tula uplift, northwestern China: Evidence for regional tectonism of the northern Tibetan Plateau, *Geol. Soc. Am. Bull.*, *115*, 35–47.
- Royden, L. H. (1996), Coupling and decoupling of crust and mantle in convergent orogens: Implications for strain partitioning in the crust, *J. Geophys. Res.*, *101*(8), 17,679–17,705.
- Ruddiman, W. F., W. L. Prell, and M. E. Raymo (1989), Late Cenozoic uplift in southern Asia and the American west: Rationale for general circulation modeling experiments, *J. Geophys. Res.*, *94*, 18,379–18,391.
- Sato, K., Y. Liu, Z. Zhu, Z. Yang, and Y. Otofujii (2001), Tertiary paleomagnetic data from northwestern Yunnan, China: Further evidence for large clockwise rotation of the Indochina block and its tectonic implications, *Earth Planet. Sci. Lett.*, *185*, 185–198.
- Shen, Z. K., M. Wang, Y. Li, D. J. Jackson, A. Yin, D. Dong, and P. Fang (2001), Crustal deformation along the Altyn Tagh Fault system, western China, from GPS, *J. Geophys. Res.*, *106*(12), 30,607–30,621.
- Tapponnier, P., M. Mattauer, F. Proust, and C. Cassaigneau (1981), Mesozoic ophiolites, sutures, and large-scale tectonic movements in Afghanistan, *Earth Planet. Sci. Lett.*, *52*, 355–371.
- Tapponnier, P., Z. Xu, F. Roger, B. Meyer, N. Arnaud, G. Wittlinger, and J. Yang (2001), Oblique stepwise rise and growth of the Tibetan Plateau, *Science*, *294*, 1671–1677.
- Thomas, J.-C., H. Perroud, P. R. Cobbold, M. L. Bazhenov, V. S. Burtman, A. Chauvin, and I. S. Sadybakasov (1993), A paleomagnetic study of Tertiary formations from the Kyrgyz Tien-Shan and its tectonic implications, *J. Geophys. Res.*, *98*, 9571–9589.
- Thomas, J.-C., A. Chauvin, D. Gapais, M. L. Bazhenov, H. Perroud, P. R. Cobbold, and V. S. Burtman (1994), Paleomagnetic evidence for Cenozoic block rotations in the Tadjick depression (central Asia), *J. Geophys. Res.*, *99*(B8), 15,141–15,160.
- van der Woerd, J., F. J. Ryerson, P. Tapponnier, Y. Gaudemer, R. Finkel, A. S. Mériaux, M. Caffee, Z. Guoguang, and H. Qunlu (1998), Holocene left-slip rate determined by cosmogenic surface dating on the Xidatan segment of the Kunlun fault (Qinghai, China), *Geology*, *26*(268), 695–698.

- Wang, E. (1997), Displacement and timing along the northern trend of the Altyn Tagh fault zone, Northern Tibet, *Earth Planet. Sci. Lett.*, *150*, 55–64.
- Washburn, Z., J. R. Arrowsmith, G. Dupont-Nivet, and W. X. Feng (2004), Paleoseismology of the Xorkol segment of the central Altyn Tagh Fault, Xinjiang, China, *Paleoseismol. Ann. Geofis.*, in press.
- Yang, T., Z. Yang, Z. Sun, and A. Lin (2002), New Early Cretaceous paleomagnetic results from Qilian orogenic belt and its tectonic implications, *Sci. China, Ser. D*, *45*(6), 565–576.
- Yang, Z., and J. Besse (1993), Paleomagnetic study of Permian and Mesozoic sedimentary rocks from northern Thailand support the extrusion model for Indochina, *Earth Planet. Sci. Lett.*, *117*, 507–524.
- Yang, Z., V. Courtillot, J. Besse, X. Ma, L. Xing, S. Xu, and J. Zhang (1992), Jurassic paleomagnetic constraints on the collision of the North and South China blocks, *Geophys. Res. Lett.*, *19*(6), 577–580.
- Yin, A., and M. T. Harrison (2000), Geologic evolution of the Himalayan-Tibetan orogen, *Annu. Rev. Earth Planet. Sci.*, *28*, 211–280.
- Yin, A., et al. (2002), Tectonic history of the Altyn Tagh fault system in northern Tibet inferred from Cenozoic sedimentation, *Geol. Soc. Am. Bull.*, *114*, 1257–1295.
- Yokoyama, M., Y. Liu, Y. Otofujii, and Z. Yang (1999), New Late Jurassic palaeomagnetic data from the northern Sichuan basin: Implications for the deformation of the Yangtze Craton, *Geophys. J. Int.*, *139*, 795–805.
- Yokoyama, M., Y. Liu, N. Halim, and Y. Otofujii (2001), Paleomagnetic study of Upper Jurassic rocks from the Sichuan basin: Tectonic aspects for the collision between the Yangtze block and the North China block, *Earth Planet. Sci. Lett.*, *193*, 273–285.
- Yu, Q., C. Li, F. Gu, Y. Hou, and K. Zhang (2001), *Regional geologic character and field mapping in the northeast margin of Qinghai-Tibet plateau in Cenozoic (in Chinese)*, 123 pp., China Univ. of Geosci. Press, Wuhan.
- Yue, Y., B. D. Ritts, and S. A. Graham (2001), Initiation and long-term slip history of the Altyn Tagh fault, *Int. Geol. Rev.*, *43*, 1087–1093.
- Yue, Y., B. D. Ritts, S. A. Graham, J. L. Wooden, G. E. Gehrels, and Z. Zhang (2004), Slowing extrusion tectonics: lowered estimate of post-early Miocene slip rate for the Altyn Tagh fault, *Earth Planet. Sci. Lett.*, *217*(1–2), 111–122.
- Zhai, Y., and T. Cai (1984), The Tertiary system of Gansu province, in *Gansu Geology*, pp. 1–40, People's Press of Gansu, Lanzhou, China.
- Zhang, P., B.-C. Burchfiel, P. Molnar, W. Zhang, D. Jiao, Q. Deng, Y. Wang, L. Royden, and F. Song (1990), Late Cenozoic tectonic evolution of the Ningxia-Hui Autonomous Region, China, *Geol. Soc. Am. Bull.*, *102*, 1484–1498.
- Zhang, Y. Q., J. L. Mercier, and P. Vergely (1998), Extension in the graben systems around the Ordos (China), and its contribution to the extrusion tectonics of south China with respect to Gobi-Mongolia, *Tectonophysics*, *285*, 41–75.

R. F. Butler, Department of Geosciences, University of Arizona, Tucson, AZ 85721, USA. (butler@geo.arizona.edu)

G. Dupont-Nivet, Faculty of Earth Sciences, Paleomagnetic Laboratory “Fort Hoofdijk”, Utrecht University, Budapestlaan 17, 3584 CD Utrecht, Netherlands. (gdn@geo.uu.nl)

B. K. Horton, Department of Earth and Space Sciences, University of California, Los Angeles, CA 90095-1567, USA. (horton@ess.ucla.edu)

G. L. Waanders, 1475 Rancho Encinitas Drive, Encinitas, CA 92024, USA. (waanpaly@cts.com)

J. Wang, Institute of Geochemistry, Chinese Academy of Sciences, Guangzhou 510640, China. (wangjh@gig.ac.cn)

J. Zhou, Faculty of Earth Sciences, China University of Geosciences, Wuhan 430074, China. (zjy522@mail.cug.edu.cn)